Journal of Power Sources 256 (2014) 206–211

Contents lists available at ScienceDirect

Journal of Power Sources

journal homepage: www.elsevier.com/locate/jpowsour

Three-dimensional MnO_2 nanowire/ZnO nanorod arrays hybrid nanostructure for high-performance and flexible supercapacitor electrode

Songzhan Li [a,b], Jian Wen [a], Xiaoming Mo [a], Hao Long [a], Haoning Wang [a], Jianbo Wang [a,*], Guojia Fang [a,*]

[a] Key Laboratory of Artificial Micro- and Nano-structures of Ministry of Education of China, Department of Electronic Science and Technology, School of Physics and Technology, Wuhan University, Wuhan 430072, PR China
[b] School of Electronic and Electrical Engineering, Wuhan Textile University, Wuhan 430073, PR China

HIGHLIGHTS

- Binder-free flexible ZnO nanorod array/MnO_2 nanowire composite capacitor electrodes are grown on carbon cloth.
- The electrochemical performance of MnO_2 nanowire electrode is greatly enhanced with the supporting of ZnO nanorod arrays.
- The hybrid nanostructure electrode delivers a high specific capacitance of 746.7 F g^{-1} at 2 mV s^{-1}.
- The specific capacitance of ZnO nanorod/MnO_2 nanowire hybrid electrode shows only losses 6.5% after 1000 cycles.
- The hybrid electrode demonstrates excellent mechanical stability under different bending angles.

ARTICLE INFO

Article history:
Received 1 November 2013
Received in revised form
26 December 2013
Accepted 15 January 2014
Available online 24 January 2014

Keywords:
Manganese oxide nanowire
Zinc oxide nanorod array
Hybrid nanostructured electrode
Flexible
Supercapacitor

ABSTRACT

Pure MnO_2 nanowires and MnO_2 nanowire/ZnO nanorod array hybrid nanostructure grown on carbon cloth are synthesized through a low temperature solution method for flexible and high performance supercapacitor applications. The MnO_2 nanowire/ZnO nanorod hybrid nanostructured electrodes exhibit more than two times higher specific capacitance, and better capacitance retention than those of pure MnO_2 nanowire electrodes. For the three-dimensional MnO_2 nanowire/ZnO nanorod array hybrid electrode, a high specific capacitance of 746.7 F g^{-1} (areal capacitance ~41.5 mF cm^{-2}) is obtained at a scan rate of 2 mV s^{-1}, while the specific capacitance of pure MnO_2 nanowire electrode is 319.6 F g^{-1}. The electrochemical impedance spectroscopy measurements also confirm MnO_2 nanowire/ZnO nanorod array hybrid electrode has better electrochemical character. The MnO_2 nanowire/ZnO nanorod array hybrid electrode shows great cycle stability, it only losses 6.5% of the initial capacitance after 1000 cycles. The energy density and power density of the hybrid electrode at 2 A g^{-1} are 63.1 Wh kg^{-1} and 950 W kg^{-1}, respectively. It is illustrated that the electrochemical performance of MnO_2 nanowire electrode has been greatly enhanced with the supporting of ZnO nanorod arrays.

1. Introduction

With the increasing power and energy demand in applications ranging from portable electronics to hybrid electric vehicles, it is essential for the utilization of clean and renewable energy. Of the various power source devices, supercapacitors have attracted considerable attention because of their unique characteristics, such as high power density, fast charge/discharge rates, and long cyclic life [1–3]. Many noble or transition metal oxides can show pseudocapacitive behavior [4–7]. Among these transition metal oxides, manganese oxides (MnO_2) are regarded as one of the most candidated electrode materials for supercapacitors due to its high theoretical specific capacitance (~1370 F g^{-1}), natural abundance, environmental friendliness and low cost [8,9]. However, the poor conductivity (~10^{-5} to 10^{-6} S cm^{-1}) of MnO_2 is a crucial factor to limit its electrochemical performance [10]. Additionally, the textural characteristics and crystal forms of MnO_2 also affect the electrochemical performances [11,12]. To produce the best possible performances of MnO_2, great efforts have been devoted in designing and developing the new framework of electrode

* Corresponding authors.
E-mail address: gjfang@whu.edu.cn (G. Fang).

0378-7753/$ – see front matter © 2014 Elsevier B.V. All rights reserved.
http://dx.doi.org/10.1016/j.jpowsour.2014.01.066

material. One effective and straightforward approach is to exploit binary or ternary composites based on MnO_2/electrical conductive materials [13–16].

Novel three-dimensional hybrid nanostructured electrodes based on one-dimensional nanowire/nanorod arrays have attracted considerable attentions due to the synergic effect of three-dimensional nanostructures. One-dimensional nanorod arrays could not only serve as a conducting scaffold for supporting electrochemically active materials, but also serve as effective channels for electrons transport [17,18]. Some hybrid nanostructures of TiO_2/MnO_2 [19], CoO/NiHON [20], CNT/RuO_2 [21], MnO_2/RGO/CNT [22] have been investigated for supercapacitor applications and improved performances have been obtained.

ZnO nanowire/nanorod is one of the most attractive functional semiconductor materials and has a small capacity, so it can function as efficient mechanical support and electron conducting pathway because of its high chemical stability, conductivity, and mechanical flexibility. Mao's group has reported ZnO@MnO_2 core@shell nanostructure electrode on titanium substrate, and obtains specific areal capacitances of be 31.30 mF cm^{-2} [17]. Yang et al. has fabricated ZnO@MnO_2 core–shell nanocables, and it authentically improves the electrochemical performance of supercapacitor electrode by high temperature annealing and hydrogenating treatment [23].

In this paper, we demonstrate a novel binder-free and flexible supercapacitor electrode with only low temperature hydrothermal in situ grown processes. Three-dimensional MnO_2 nanowire/ZnO nanorod hybrid nanostructured arrays are in situ grown by hydrothermal processes on carbon cloth. The carbon cloth provides a good electrical conductive path and a light, flexible, and stable substrate for composites growth. As a binder-free flexible electrode for supercapacitor, the MnO_2 nanowire/ZnO nanorod array hybrid electrode exhibits a very high specific capacitance of 746.7 F g^{-1} (areal capacitance ~41.5 mF cm^{-2}) and good cycling stability.

2. Experimental

Carbon cloth with high flexibility and high electrical conductivity is used as a current collector for conformal coating of nanostructured composites for supercapacitor electrode without any insulating binders. The whole fabrication procedures of nanostructured composite electrodes are schematically illustrated in Fig. 1. ZnO nanorod arrays are grown on carbon cloth substrate by a seed-assisted hypothermal method. The nutrient solution is an aqueous solution of 0.025 M zinc nitrate [$Zn(NO_3)_2 \cdot 6H_2O$] and hexamethylenetetramine, then the reaction is kept at 130 °C for 2 h. Before growing the ZnO nanorod arrays, a 200 nm ZnO seed layer is deposited on carbon cloth. MnO_2 nanowires are synthesized from a neutral precursor solution (pH 7) of Na_2SO_4 and $KMnO_4$ mixture solutions. 0.1 g Na_2SO_4 is dissolved in 20 mL deionized water, and

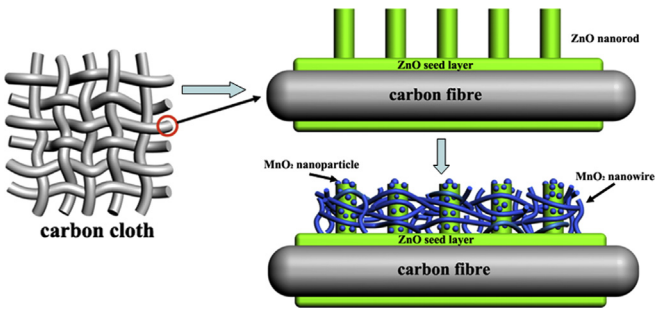

Fig. 1. Schematic diagram illustrating the fabrication process for three-dimensional MnO_2 nanowire/ZnO nanorod array hybrid nanostructure on carbon cloth.

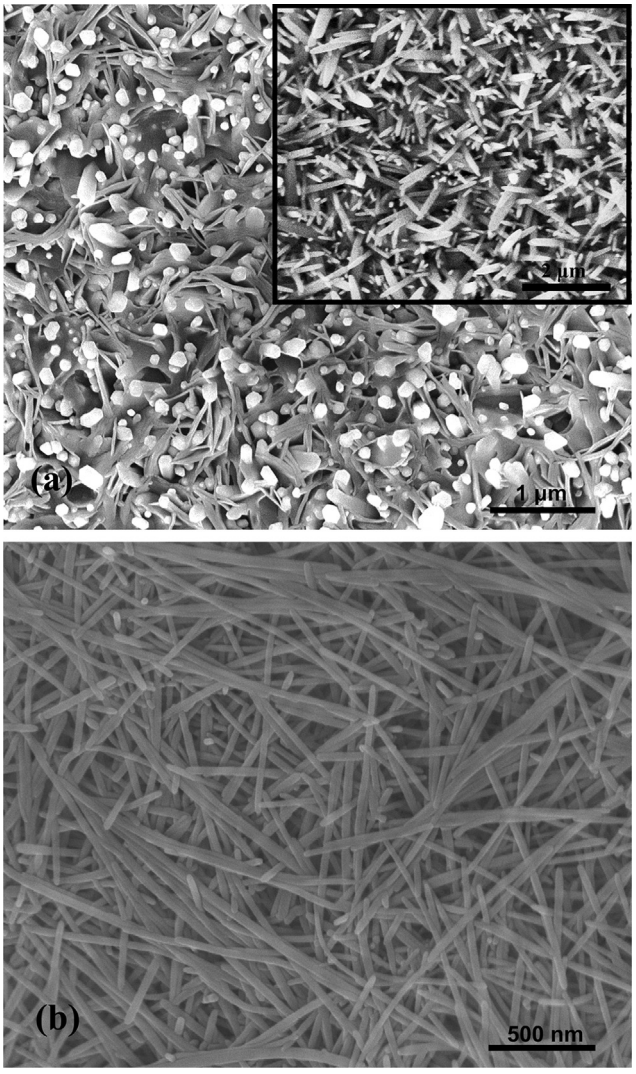

Fig. 2. (a) SEM image of ZnO nanorod array with MnO_2 nanowires, the inset is a magnification SEM image of pure ZnO nanorod arrays. (b) SEM morphology of MnO_2 nanowires.

then 20 mL $KMnO_4$ (0.03 g mL^{-1}) solution is added drop by drop into it and stirs for 60 min to obtain a homogeneous solution. Subsequently, the well-mixed solution is transferred into a 60 mL autoclave. The pre-prepared ZnO nanorod arrays/carbon cloth and carbon cloth substrates are put into the autoclave and stores in the sealed autoclave keeping at 160 °C in an oven for 6 h. After the autoclave cooling to the room temperature, the substrates are taken out and washed several times with deionized water, and then dried at 50 °C for 4 h. The mass of active materials is calculated from the weight difference before and after the synthesis process. The loading amount of active materials is approximately 0.2 mg.

The morphologies are characterized by high-resolution field emission scanning electron microscopy (SEM, Nova Nano-SEM 450, FEI). The crystal structures of electrode materials are characterized by X-ray diffraction (XRD, Bruker Axs, D8 Advance) with Cu Kα radiation. The chemical compositions of the composites are investigated using X-ray photoelectron spectroscopy (XPS, ESCLAB 250Xi, Thermo Scientific).

The electrochemical measurements are carried out in a three-electrode testing system (CHI 660E electrochemical workstation, Chenhua, Shanghai) with a platinum foil as counter electrode and saturated calomel electrode (SCE) as reference electrode in 1 M

Na_2SO_4 electrolyte solution. The galvanostatic charge–discharge tests are conducted on a LAND battery program-control test system (LAND CT-2001A) at room temperature.

3. Results and discussion

The morphologies of MnO_2 and ZnO nanorod composites are imaged by SEM. SEM image of ZnO nano arrays (inset of Fig. 2a) indicates that the ZnO nanorods are needle-like nanostructure having diameters of 50–150 nm. Fig. 2a displays SEM image of ZnO nanorod arrays with MnO_2 nanowires, and the composite shows a three-dimensional cross-linked nano-scale network structure. Comparing with the needle-like ZnO nanorods, it is found that the tops of MnO_2 nanowire/ZnO nanorod array nano-composite present cap-shaped. The possible reason is that the top of ZnO nanorod is covered by some MnO_2 nano particles during the growth of MnO_2 nanowires. As shown in Fig. 2b, MnO_2 nanowires are homogeneous with a mean diameter of 30 nm and length of several micrometers, and have smooth and clean surfaces.

XPS is used to provide further evidence for the successful synthesis of ZnO nanorod/MnO_2 composite, and the Mn 2p, Zn 2p and O 1s spectra are presented in Fig. 3. As shown in Fig. 3a, there are two peaks centered at 642.0 and 653.8 eV in the Mn 2p spectrum with a spin-energy separation of 11.8 eV, demonstrating the binding energy of Mn $2p_{3/2}$ and Mn $2p_{1/2}$, respectively, which reveals Mn^{4+} ions are dominant in the composites [24]. The XPS spectrum of Zn is displayed in Fig. 3b. It can be seen that the XPS peak positions of Zn $2p_{3/2}$ and Zn $2p_{1/2}$ are centered at about 1021.7 and 1044.9 eV, respectively, corresponding to Zn^{2+} species. For the O 1s XPS spectrum, the original curve can be best fitted with two peaks by Gaussian. The lower energy peak located at 531.1 eV is assigned to the coordination of oxygen in Mn–O–Mn [25], while the higher energy peak centered at 532.6 eV corresponds to the O–Zn binding [26]. Therefore, the above results confirmed the existence of MnO_2 and ZnO in the composites. The XRD analysis also demonstrates that the crystalline phases of MnO_2 and ZnO coexist in hybrid electrode materials (See Supporting information).

The as-prepared MnO_2 nanowires and MnO_2 nanowire/ZnO nanorod array nano-composite grown on carbon cloth substrate are further evaluated as electrode materials for supercapacitors. Fig. 4a shows the cyclic voltammetry (CV) curves of pure MnO_2 nanowires and MnO_2 nanowire/ZnO nanorod array hybrid electrodes at a fixed scan rate of 100 mV s^{-1}. These curves exhibit roughly rectangular mirror images. Compared to that of pure MnO_2 nanowire electrode, CV curve of MnO_2 nanowire/ZnO nanorod array nano-composite has a larger integrated CV area and exhibits a very rapid current response on voltage reversal at each end potential and possesses high reversibility, meaning excellent electrochemical performance. The electrochemical characteristics of the MnO_2 nanowire/ZnO nanorod array hybrid electrode are examined by changing the scan rate with potential windows ranging from 0 to 0.9 V, and the results are shown in the inset of Fig. 4b. It is clearly demonstrated that all of the CV curves are almost quasi-rectangular with symmetric shape, suggesting that composite electrodes with fast, reversible reaction and an ideal capacitive behavior have been obtained.

The specific capacitances (C) are calculated from the CV curves according to the following equation [27]:

$$C = \frac{\int I \cdot dV}{m \cdot v \cdot \Delta V}$$

where I is the response current (A), m is the mass of active electrode material (g), v is the potential scan rate (V s^{-1}), and ΔV is the potential window (V). Fig. 4b shows comparative specific capacitances

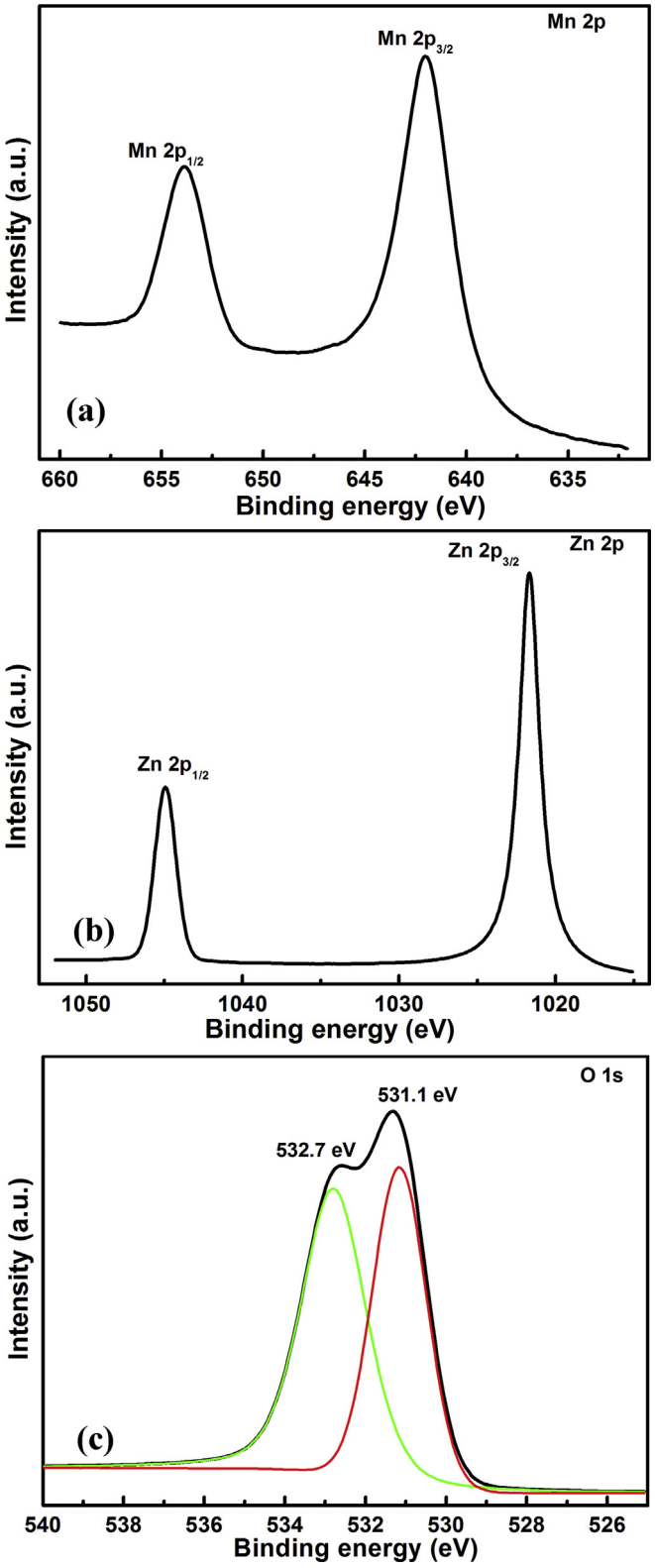

Fig. 3. (a) Mn 2p, (b) Zn 2p and (c) O1s XPS spectra of MnO_2 nanowire/ZnO nanorod array hybrid composite.

of pure MnO_2 nanowires and MnO_2 nanowire/ZnO nanorod array nano-composite calculated from CV curves at voltage scan rates from 2 to 200 mV s^{-1}, as well as that of pure ZnO nanorod arrays. The specific capacitance of ZnO nanorod arrays is 40 F g^{-1} at a scan

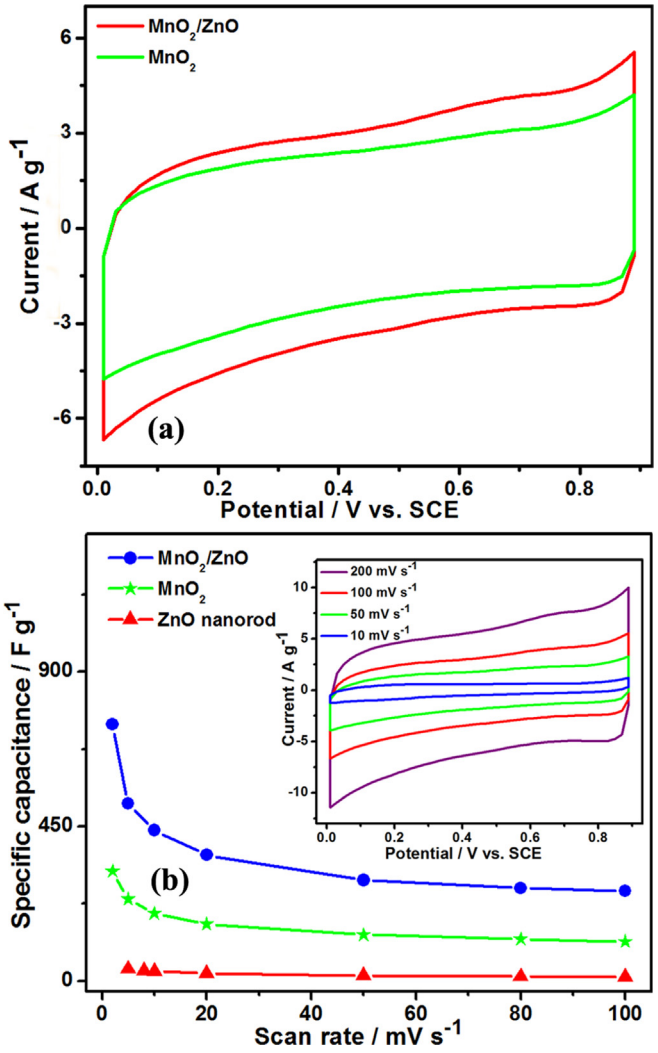

Fig. 4. (a) CV curves of pure MnO_2 nanowire and MnO_2 nanowire/ZnO nanorod array hybrid electrodes at a fixed scan rate of 100 mV s^{-1}. (b) Specific capacitances of pure MnO_2 nanowire and MnO_2 nanowire/ZnO nanorod array hybrid electrodes at voltage scan rates from 2 to 200 mV s^{-1}, as well as that of pure ZnO nanorod array electrode. The inset is CV curves of MnO_2 nanowire/ZnO nanorod array hybrid electrodes at different scan rate with potential windows ranging from 0 to 0.9 V.

rate of 2 mV s^{-1}, which is comparable to the reported values in literature [28,29]. It is obvious that MnO_2 nanowire/ZnO nanorod array nano-composite exhibits higher rate performance than pure MnO_2 nanowires. The MnO_2 nanowire/ZnO nanorod array hybrid electrode achieves a higher specific capacitance of 746.7 F g^{-1} (areal capacitance ~41.5 mF cm^{-2}) at the scan rate of 2 mV s^{-1}, which exhibits more than twice higher than that of pure MnO_2 nanowire electrode (~319.6 F g^{-1}). At a high scan rate of 100 mV s^{-1}, the specific capacitance of MnO_2 nanowire/ZnO nanorod array nano-composite is 261.5 F g^{-1}, and the pure MnO_2 nanowire electrode only yields 120 F g^{-1}. The decrease of specific capacitance with increasing scan rate can be ascribed to the reduced diffusion time for insertion/extraction of protons or alkali cations into birnessite-type MnO_2 at high scan rate. The introduction of ZnO nanorod arrays and three-dimensional hybrid structures significantly enhances the electrochemical performance of MnO_2.

The long-term cycle stability is one of the most critical factors in supercapacitor applications. The cycling measurement for MnO_2 nanowire/ZnO nanorod array hybrid electrode was carried out with a scan rate of 100 mV s^{-1} for 1000 cycles. Some representative CV curves of composite electrode are presented in the inset of Fig. 5a, and all the curves are almost overlapping with each other. Fig. 5a shows the resulting specific capacitance retention as a function of cycle numbers. It is found that the hybrid electrode exhibits good stability over the entire cycle numbers. The specific capacitance of the hybrid electrode only losses 6.5% of the initial capacitance after 1000 cycles, indicating great cycle stability. The decrease of specific capacitance could be attributed to the partial dissolution of MnO_2 by the formation of soluble Mn^{2+} ions [30].

Significantly, the CV curves in Fig. 5b collected from the MnO_2 nanowire/ZnO nanorod array hybrid electrode under different bending angles still keep quasi-rectangular and symmetric in shape. The change of shape for CV curves seems to be subtle and acceptable, demonstrating its excellent mechanical stability as flexible energy storage devices.

The electrochemical impedance spectroscopy (EIS) measurements are employed to further evaluate the electrochemical properties of pure MnO_2 nanowire electrode and MnO_2 nanowire/ZnO nanorod array hybrid electrode. Fig. 6a shows the Nyquist plots of these electrodes, which consist of semicircle arcs at high-to-

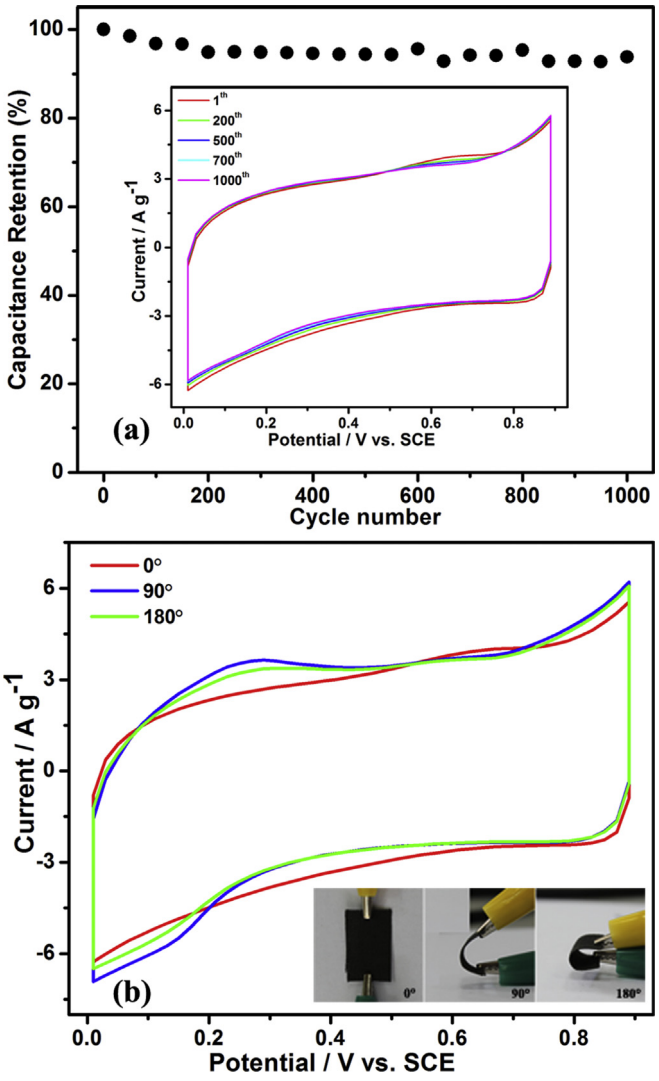

Fig. 5. (a) Capacitance retention as a function of cycle numbers, the inset is some representative CV curves of composite electrode at a scan rate of 100 mV s^{-1}. (b) CV curves of MnO_2 nanowire/ZnO nanorod array hybrid electrode under different bending angles at a scan rate of 100 mV s^{-1}, the insets are the pictures of hybrid electrode under different bending angles.

middle frequency region and straight lines at low frequency range. The EIS data can be fitted by an equivalent circuit consisting of the bulk electrolyte resistance (R_s), the charge transfer resistance (R_{ct}), the resistance related to the ion diffusion in electrolyte (R_w), and the electrochemical capacitance (C_F). Seeing from the Nyquist plots, the R_s and R_{ct} of MnO_2 nanowire/ZnO nanorod array hybrid electrode are smaller than that of pure MnO_2 nanowire electrode, which may due to the poor electrical conductivity of MnO_2. In addition, it is obviously that the slope of MnO_2 nanowire/ZnO nanorod array hybrid electrode is larger than pure MnO_2 nanowire electrode, indicating the hybrid electrode has better electrochemical character.

All of the above results confirm that such a design of MnO_2 nanowire/ZnO nanorod array nano-composite/carbon cloth allows maximizing the performance of MnO_2, and this may be attributed to the following reasons: (i) three-dimensional MnO_2 nanowire/ZnO nanorod hybrid nanostructured arrays possess larger specific surface area than that of pure MnO_2 nanowire, which could result in higher capacitance; (ii) in such a unique coaxial nanostructure, the ZnO nanorods also serve as electrical conductive pathways for fast charge collection and transfer [31]; (iii) during the charge storage process, the MnO_2 nanowires provide short pathways for ion/electron transport; (iv) the porous network structure originated in MnO_2 nanowires enables fast electrolyte penetration and facilitates continuous ion/electron transport throughout the electrode; (v) the binder-free electrode enables a fast electrochemical reaction rate.

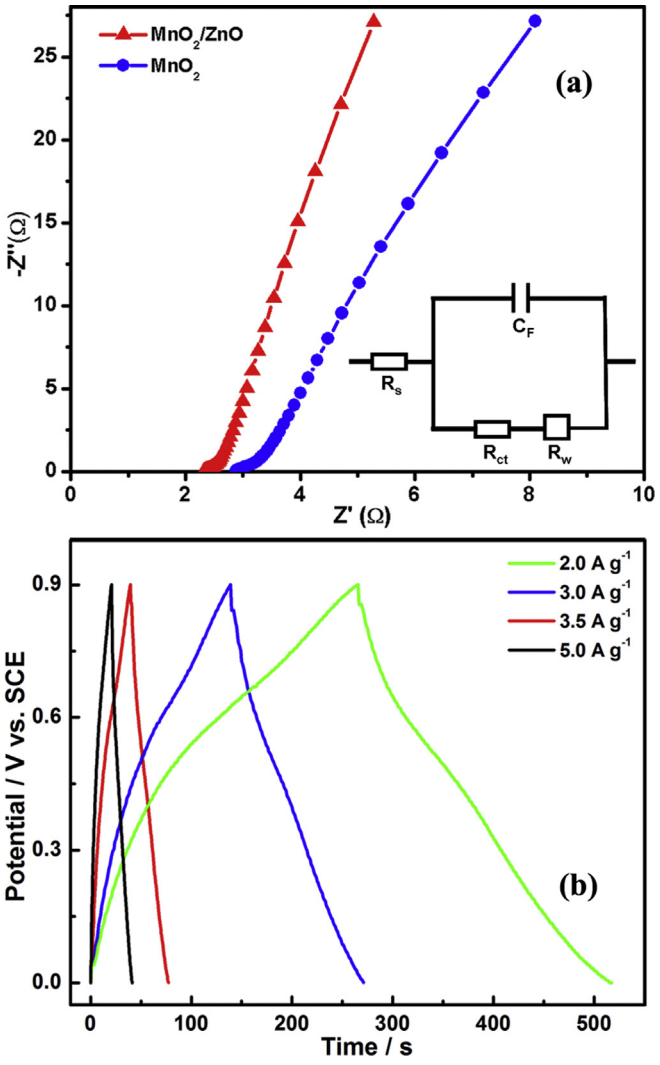

Fig. 6. (a) The Nyquist plots of pure MnO_2 nanowire electrode and MnO_2 nanowire/ZnO nanorod array hybrid electrode. The inset is the equivalent circuit. (b) The galvanostatic charge–discharge curves of MnO_2 nanowire/ZnO nanorod array hybrid electrodes at various current densities.

The galvanostatic charge–discharge curves of MnO_2 nanowire/ZnO nanorod array hybrid electrode at current density of 2.0, 3.0, 3.5, and 5.0 A g^{-1} were shown in Fig. 6b. The charge–discharge curves display a symmetric shape, indicating that the composite has outstanding supercapacitive behavior and there is a highly superior reversible Faradaic reaction between Na^+ and nano-MnO_2. The specific capacitance can be calculated from the discharging curve based on the equation [28]:

$$C = \frac{I \cdot \Delta t}{m \cdot \Delta V}$$

where I is the constant discharge current (A), Δt is the discharging time (s), m is the total mass of active materials in electrode (g), and ΔV is the voltage drop upon discharging (V). The specific capacitance obtained from the discharging curves is calculated to be 501.1 F g^{-1} at a current density of 2 A g^{-1}, which is almost comparable with the specific capacitance 516.4 F g^{-1} calculated from the CV measurements at a scan rate of 10 mV s^{-1}.

The power density and energy density can be estimated from the discharging curves using the following equations [27]:

$$E = \frac{1}{2} C \Delta V^2$$

$$P = \frac{E}{\Delta t}$$

At a high current density of 2 A g^{-1}, the calculated energy density of the ZnO nanorod array/MnO_2 nanowire hybrid electrode is 63.1 Wh kg^{-1} and the average power density is 950 W kg^{-1}. It suggests that this MnO_2 nanowire/ZnO nanorod array nanocomposite has potential application for supercapacitor.

4. Conclusions

Three-dimensional MnO_2 nanowire/ZnO nanorod array hybrid nanostructure grown on carbon cloth has been demonstrated for flexible supercapacitor electrode applications, and such binder-free electrodes demonstrate a high electrochemical performance. The high specific capacitance reaches 746.7 F g^{-1} at a scan rate of 2 mV s^{-1}, and it possesses high energy density with good long-term cyclic stability. What's more, the performance of MnO_2 nanowire/ZnO nanorod array hybrid electrode under different bending angles demonstrates excellent mechanical stability as flexible energy storage devices. EIS data also demonstrates the electrochemical performance of MnO_2 nanowires can be greatly promoted by the supporting of ZnO nanorods. Three-dimensional MnO_2 nanowire/ZnO nanorod array hybrid nanostructure is expected to hold great promise as a high-performance electrode material for flexible supercapacitors.

Acknowledgments

This work was supported by the 973 Program (2011CB933300) of China, the National Natural Science Foundation of China (11074194, 61376013), the Natural Science Foundation of Jiangsu Province (BK20131186), and Wuhan Science & Technology Bureau (2013010501010141).

Appendix A. Supplementary data

Supplementary data related to this article can be found at http://dx.doi.org/10.1016/j.jpowsour.2014.01.066.

References

[1] C.W. Shen, X.H. Wang, S.W. Li, J.G. Wang, W.F. Zhang, F.Y. Kang, J. Power Sources 234 (2013) 302–309.
[2] S. Xin, Y.G. Guo, L.J. Wan, Acc. Chem. Res. 45 (2012) 1759–1769.
[3] H. Jiang, C. Li, T. Sun, J. Ma, Chem. Commun. 48 (2012) 2606–2608.
[4] Z.C. Xing, Q.X. Chu, X.B. Ren, C.J. Ge, A.H. Qusti, A.M. Asiri, A.O. Al-Youbi, X.P. Sun, J. Power Sources 245 (2014) 463–467.
[5] J. Jiang, Y. Li, J. Liu, X. Huang, C. Yuan, X. Lou, Adv. Mater. 24 (2012) 5166–5180.
[6] Z. Tang, C.H. Tang, H. Gong, Adv. Funct. Mater. 22 (2012) 1272–1278.
[7] G. Zhang, H. Wu, H. Hoster, M. Chan-Park, X. Lou, Energy Environ. Sci. 5 (2012) 9453–9456.
[8] G.P. Xiong, K.P.S.S. Hembram, R.G. Reifenberger, T.S. Fisher, J. Power Sources 227 (2013) 254–259.
[9] Z.P. Li, J.Q. Wang, S. Liu, X.H. Liu, S.R. Yang, J. Power Sources 196 (2011) 8160–8165.
[10] Z. Yu, B. Duong, D. Abbitt, J. Thomas, Adv. Mater. 25 (2013) 3302–3306.
[11] J.G. Wang, Y. Yang, Z.H. Huang, F.Y. Kang, Electrochim. Acta 56 (2011) 9240–9247.
[12] J.H. Kim, K.H. Lee, L.J. Overzet, G.S. Lee, Nano Lett. 11 (2011) 2611–2617.
[13] Y. Jin, H.Y. Chen, M.H. Chen, N. Liu, Q.W. Li, ACS Appl. Mater. Interfaces 5 (2013) 3408–3416.
[14] X.C. Dong, X.W. Wang, J. Wang, H. Song, X.G. Li, L.H. Wang, M.B. Chan-Park, C.M. Li, P. Chen, Carbon 50 (2012) 4865–4870.
[15] J. Yan, E. Khoo, A. Sumboja, P.S. Lee, ACS Nano 4 (2010) 4247–4255.
[16] Jaidev, R.I. Jafri, A.K. Mishra, S. Ramaprabhu, J. Mater. Chem. 21 (2011) 17601–17605.
[17] X. Sun, Q. Li, Y.N. Lü, Y.B. Mao, Chem. Commun. 49 (2013) 4456–4458.
[18] D. Sarkar, G.G. Khan, A.K. Singh, K. Mandal, J. Phys. Chem. C 117 (2013) 15523–15531.
[19] X.H. Lu, M.H. Yu, G.M. Wang, T. Zhai, S.L. Xie, Y.C. Ling, Y.X. Tong, Y. Li, Adv. Mater. 25 (2013) 267–272.
[20] C. Guan, J. Liu, C. Cheng, H. Li, X. Li, W. Zhou, H. Zhang, H.J. Fan, Energy Environ. Sci. 4 (2011) 4496–4499.
[21] J.S. Ye, H.F. Cui, X. Liu, T.M. Lim, W.D. Zhang, F.S. Sheu, Small 1 (2005) 560–565.
[22] Z.B. Lei, F.H. Shi, L. Lu, ACS Appl. Mater. Interfaces 4 (2012) 1058–1064.
[23] P.H. Yang, X. Xiao, Y.Z. Li, Y. Ding, P.F. Qiang, X.H. Tan, W.J. Mai, Z.Y. Lin, W.Z. Wu, T.Q. Li, H.Y. Jin, P.Y. Liu, J. Zhou, C.P. Wong, Z.L. Wang, ACS Nano 7 (2013) 2617–2626.
[24] M. Toupin, T. Brousse, D. Bélanger, Chem. Mater. 16 (2004) 3184–3190.
[25] L.Y. Yuan, X.H. Lu, X. Xiao, T. Zhai, J.J. Dai, F.C. Zhang, B. Hu, X. Wang, L. Gong, J. Chen, C.G. Hu, Y.X. Tong, J. Zhou, Z.L. Wang, ACS Nano 6 (2011) 656–661.
[26] C.C. Li, X.M. Yin, Q.H. Li, T.H. Wang, CrystEngComm 13 (2011) 1557–1563.
[27] K. Liang, X.Z. Tang, W.C. Hu, J. Mater. Chem. 22 (2012) 11062–11067.
[28] G.L. Guo, L. Huang, Q.H. Chang, L.C. Ji, Y. Liu, Y.Q. Xie, W.Z. Shi, N.Q. Jia, Appl. Phys. Lett. 99 (2011) 083111.
[29] K.K. Purushothaman, V.S. Priya, S. Nagamuthu, S. Vijayakumar, G. Muralidharan, Micro Nano Lett. 6 (2011) 668–670.
[30] J. Yan, Z.J. Fan, T. Wei, J. Cheng, B. Shao, K. Wang, L.P. Song, M.L. Zhang, J. Power Sources 194 (2009) 1202–1207.
[31] J.G. Wang, Y. Yang, Z.H. Huang, F.Y. Kang, Electrochim. Acta 75 (2012) 213–219.